



Portable spectral profiler probe for rapid snow grain size stratigraphy

Daniel F. Berisford ^{a,*}, Noah P. Molotch ^{a,b}, Michael T. Durand ^c, Thomas H. Painter ^a

^a Jet Propulsion Laboratory, California Institute of Technology, 4800 Oak Grove Dr., Pasadena, CA 91109, USA

^b Institute of Arctic and Alpine Research, Dept. of Geography, University of Colorado at Boulder, 1560 30th Street, Boulder, CO 80303, USA

^c School of Earth Sciences, The Ohio State University, 275 Mendenhall Laboratory, 125 South Oval Mall, Columbus, OH 43210, USA

ARTICLE INFO

Article history:

Received 19 March 2012

Accepted 5 September 2012

Keywords:

Snow
Grain size
Spectroscopy
Field instrument

ABSTRACT

We present a portable spectral profiler probe to measure snow grain size stratigraphy in mountain snowpack at up to 5 mm vertical resolution, without the need for snow pit excavation. The probe infers grain size using near-infrared reflectance spectroscopy by inserting into the snowpack an optical package consisting of a light source and fiber optic receiver, which views the snow laterally and sends the collected reflected light to a spectrometer at the surface. The instrument can be easily dismantled and transported in a backpack, and rapidly deployed in the field. Grain size profiles from the probe, along with snow-pit contact spectroscopy and hand lens measurements were gathered and compared during winter and spring 2010 field campaigns in Colorado. Results from the probe agree to within 30% with snow-pit contact spectroscopy measurements, except when thin layers are present, which are detected at better vertical resolution by the profiler probe. The results highlight the lateral heterogeneity inherent in most mountain snowpacks, which is impractical to measure with conventional techniques. This type of measurement, along with density measurements, can greatly impact the accuracy of remote passive and active microwave retrievals.

© 2012 Elsevier B.V. All rights reserved.

1. Introduction

Snowmelt from mountainous regions provides more than 70% of fresh water for the western United States and represents the dominant water source for 60 million Americans and over one billion people globally (Bales et al., 2006; National Research Council, 2007). Snowpack in low to mid-latitude mountain ranges is highly affected by global and local climate changes, including temperature variations and particulate pollutants from industrial sources and windblown dust (Flanner et al., 2007; Flanner et al., 2009; Painter et al., 2007a). The remote sensing community is actively pursuing techniques with the ultimate goal of measuring all relevant snowpack properties from orbital platforms, to enable the study of worldwide climate patterns and their effect on local snow levels and water availability.

Current technologies for observing snow remotely include synthetic aperture radar (Rott et al., 2010; Shi and Dozier, 2000), passive microwave radiometers (Chang et al., 1982; Durand and Margulis, 2006; Foster et al., 1997, 2005; Kelly et al., 2003), and space-borne and airborne multispectral and hyperspectral optical sensors (Dozier et al., 2009; Nolin, 2010). Several space missions and airborne radar campaigns will provide data that can be significantly improved and enable greater understanding of terrestrial snow and ice when combined with in-situ measurements of grain size stratigraphy. Among these are the NASA ICESat II (Ice, Cloud, and land Elevation Satellite-2), AMSR2

(Advanced Microwave Scanning Radiometer 2), and the European Space Agency's CoReH2O (Cold Regions Hydrology High-resolution Observatory).

Many of these measurements are acutely sensitive to snow grain size stratigraphy (Brucker et al., 2011) and spatial variation, yet the effect on the observed signals is not well understood (Durand et al., 2008a, 2008b). Thus, the range of measurements across the electromagnetic spectrum requires ground measurements of grain size for accurate data interpretation. To fully understand the radiative and convective energy balance in snowy regions, large datasets of ground-based grain size measurements are needed (Langlois et al., 2010). This is only possible with new techniques allowing for much more rapid acquisition than previously available.

Current techniques for measuring grain size include more direct observations such as hand lens estimation (American Avalanche Association, 2004; Fierz et al., 2009), stereology (Matzl and Schneebeli, 2010), and X-ray tomography (Brzoska et al., 2001; Chen and Baker, 2010). Optical or indirect methods include near infrared photography (Matzl and Schneebeli, 2006), laser reflectance with an integrating sphere (Gallet et al., 2009), and contact spectroscopy (Painter et al., 2007b). Additionally, methane absorption provides a measure of specific surface area (Kerbrat et al., 2008; Legagneux et al., 2002). All of these techniques require excavation of a snow pit, which can significantly disturb the snowpack and require an hour to days of labor to obtain a single sample of grain size stratigraphy. This sample is then extrapolated spatially to the scale of a remote sensing ground instantaneous field of view (e.g. 25–40 km for passive microwave) with unknown but likely great uncertainty, given the spatial variability of deposition/

* Corresponding author. Tel.: +1 626 318 3861.

E-mail address: daniel.berisford@jpl.nasa.gov (D.F. Berisford).

redistribution of snow and energy fluxes to that snow column (Marshall et al., 2007).

A more applicable length scale for radiative transfer through snow is the optical equivalent grain diameter (OGD), defined as the diameter of a spherical pure ice grain which gives close approximation of hemispherical fluxes compared to observed fluxes (Grenfell and Warren, 1999). A more precise physical description for understanding the dimensions that impact radiation within the snow column (given that snow is generally a sintered medium and not usually a collection of distinct particles) can be given in terms of specific surface area (SSA), which is the surface area per unit mass of the grain (Domine et al., 2008; Warren, 1982). Under the assumption of spherical particles, the relationship between OGD and SSA is given by:

$$\text{OGD} = \frac{6}{\rho \cdot \text{SSA}} \quad (1)$$

where ρ is the snow mass density.

NIR photography, laser reflectance with an integrating sphere, and contact spectroscopy are optical techniques that infer the OGD by NIR reflectance from the wall of a snow pit. NIR photography uses absolute reflectance in the 840–940 nm wavelength band to estimate grain size simultaneously for every pixel in the image of the pit wall, providing high (~1 mm) horizontal and vertical spatial resolution (Brucker et al., 2011; Langlois et al., 2010; Matzl and Schneebeli, 2006). SSA is calculated from an empirical relationship between NIR reflectance and stereology SSA measurements. This technique requires great care in preparation of the pit face, camera setup, and lighting conditions, but for shallow pits can be performed very rapidly.

The DUFISSS instrument (Gallet et al., 2009) uses an integrating sphere to measure hemispherical reflectance from an NIR laser from snow samples collected from a snow pit wall. This provides highly repeatable measurements under controlled conditions, but requires snow pit excavation and sample removal. Moreover, the DUFISSS' technique requires an empirical correction due to the contamination of signal by the sampling dish when samples are optically thin.

NIR contact spectroscopy uses a broadband illumination source and a fiber optic pickup mounted in a handheld probe that is placed in near contact with the pit face with 2 cm vertical sampling (Painter et al., 2007b). Grain size is determined by integrating an ice absorption feature with a local maximum at 1030 nm and comparing the integral to that obtained from ideal spectra from a radiative transfer model for spherical grains (Nolin and Dozier, 2000; Painter et al., 2007b; Stamnes et al., 1988). The stratigraphic profile is obtained by stepping the probe incrementally down the pit face.

Although highly advanced, all of these techniques require snow pit excavation, which requires significant labor to obtain a single profile. One recent and promising prototype instrument has been developed to measure grain size without snow pit excavation (Arnaud et al., 2011). The POSSSUM device uses a powered drill to bore a hole into glacial snow/firn, into which a mechanical winch lowers the instrument. The instrument uses reflection from a single-frequency laser to obtain SSA, and a second frequency laser to measure distance to the surface. This presents an attractive means to measure deep profiles in glacial environments and other deep snowpacks. However, for snowpacks of moderate depths and in mountainous terrain, a smaller, more portable instrument can facilitate rapid acquisition of many profiles in a given area.

We have developed a prototype lightweight, portable probe that performs contact spectroscopy measurements in-situ, by inserting an optical probe into the snowpack instead of digging a pit. It should be noted that the grain size measurement technique presented here is not new. The probe is an application of the existing technique of contact spectroscopy in a novel delivery package, which enables the collection of data at least an order of magnitude faster than snow-pit techniques, and lessens disturbance to the measurement of grain size by avoiding

exposing the underlying snow grains to the atmosphere and direct or once-reflected sunlight. In the following sections we present the design and construction of the prototype, along with results from testing against snow-pit contact spectroscopy and hand lens measurements from winter and spring field campaigns in Colorado.

2. Methods

2.1. Probe mechanical design

The basic design of the probe consists of a hollow aluminum sleeve that is inserted vertically into a hole in the snowpack, an optical package that is lowered inside the sleeve, and an above-ground manual clamping and drive mechanism for raising and lowering the optical package. The probe irradiates the snow surface laterally (orthogonal to the probe axis) with a broadband shortwave source (useful wavelength range 300 nm to 2500 nm) through slits in the sleeve, and a fiber-optic pickup couples the reflected light from the snow into an optical fiber that carries the signal out to a spectrometer on the surface which records the reflected spectrum.

Fig. 1 shows diagrams of in-bore and aboveground components of the instrument. The sleeve consists of a standard, 41 mm inner-diameter Federal snow sampler (www.unionforge.com), assembled in sections, that has been modified with a welded cap at the bottom end and milled slots of 16 mm width. These slots allow the probe to view the snow laterally from within the sleeve. An aluminum bore rider carries all of the probe optics, allowing the entire package to be moved vertically and rotated inside the sleeve by a hollow aluminum drive shaft.

At the lowermost tip of the bore rider, a cylindrical nylon “bottle brush” protrudes downward to sweep loose snow and debris from in front of the probe. A black, opaque plastic tarp of area 1 m², lain flat on the snow surface, blocks sunlight from penetrating to the probe location. The unit packs into a small backpack, with a separate pack for the spectrometer. It is possible to fit all of the hardware into a single pack with the spectrometer, however for this series of tests, we chose to keep the two packs separate to take advantage of the custom-made spectrometer pack supplied by ASD.

2.2. Optics

The optical package carried by the bore rider consists of a bifurcated fiber optic reflectance probe, an optical camera, and a halogen light source. The reflectance probe views the snow at a 28° angle of incidence through a protected gold front surface mirror, allowing it to collect reflected radiance from the snow and send it to the spectrometer at the snow surface via fiber optic cable (Fig. 2, Table 1).

The halogen light source shines onto the snow at a 52° angle of incidence and the reflected light is picked up at a 28° incidence angle, in the forward scattering direction. This light source consists of a bulb with output roughly 150 lumens (~2 W/cm²) and reflector identical to those used in the contact probe (to be discussed later), but with a slightly trimmed reflector to make it more compact. Either this light, or an external light source can be used depending on the desired configuration.

The spectrometer used for all experiments presented here is an ASD FieldSpec Pro (www.asdi.com), powered from a small 12 V battery. The unit covers the spectral range from 350 to 2500 nm with 3 nm spectral resolution at 700 nm and 10 nm resolution at 1400 nm, splined to 1 nm spectral reporting. The optical camera (Ridgid MicroExplorer inspection camera—<http://www.ridgid.com/Tools/micro-Explorer>) views the snow at approximately normal incidence through a plastic mirror, allowing a partial view of the snow at the measurement location for qualitative comparison between locations. The camera also provides a partial view of the backside of the probe mirror, and is used here for alignment purposes only.

The bifurcated fiber-optic reflectance probe is a commercially available part from Analytical Spectral Devices, Inc. (ASD) (www.asdi.com).

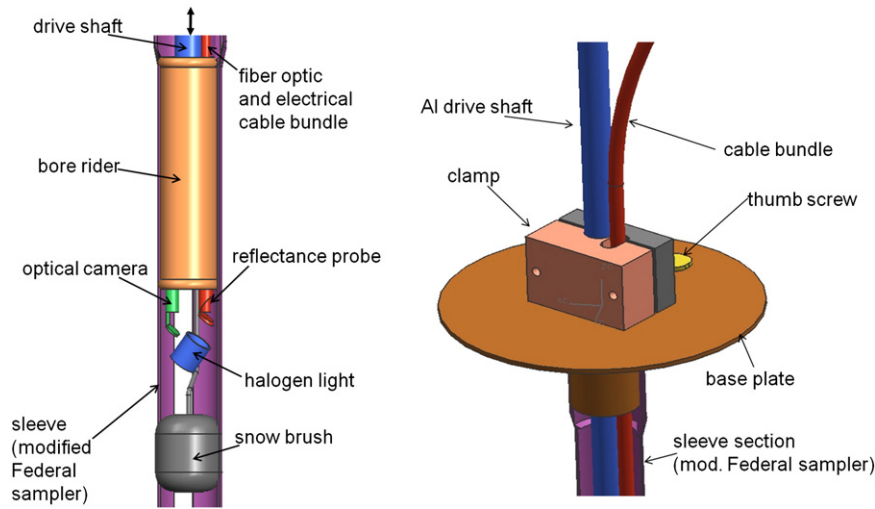


Fig. 1. CAD models: left shows in-bore components, right shows above-surface components. Note the sleeve is cutaway and rotated to show the milled slot.

com), constructed of two multi-element fiber optic cables, which merge into one at the probe tip. This allows a remote light source at the surface to be connected to one of the two bifurcated legs of the cable, with the spectrometer connected to the other leg. With this configuration, the incident and reflected light signals travel along the same path at the probe tip, with 180 degree (backscatter) reflected azimuth.

With the two different light sources, the probe can operate in two modes of illumination, hereby referred to as “fiber light” and “in-bore light” modes. With the fiber light mode, the remote halogen light source on the surface is used via one leg of the bifurcated fiber optic, and the light on the bore rider is not used. For in-bore light operation, the remote source is not used and instead the halogen bulb mounted on the probe is illuminated. Note that these two illumination conditions have significantly different angles of incidence, and the fiber light is closer to a direct beam source, while the in-bore light is a mixture of direct and diffuse light.

To fix the motion of the probe, a clamping system mounts atop a 15 cm diameter aluminum disk, which screws into the top of the uppermost section of the sleeve above the snow surface, as shown in Fig. 1. Tightening the clamp locks the drive shaft in place to fix the probe location, and loosening allows the shaft to move vertically or rotate with 1 cm resolution. The system is entirely manual and can be operated in the field by a user wearing thick gloves.

Unlike all open snow-pit techniques, the probe is much more robust in severe (especially windy and snowing) weather, as one does not have to keep snow off the pit face. The spectrometer itself can operate down to approximately $-15\text{ }^{\circ}\text{C}$ before encountering problems with an internal shutter operating properly. However, because it is enclosed in a backpack and generates a small amount of internal heating, it can be operated in colder ambient conditions.

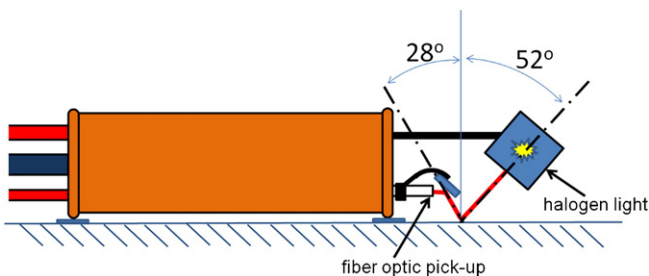


Fig. 2. Schematic of probe head optical angles.

2.3. Calibration

For calibration of the signal, a Spectralon white reference panel (<http://www.labsphere.com>) with near-unity diffuse reflectance (Bruegge et al., 2001) is held against the sleeve at the viewing location, and a black plastic tarp is draped over the unit to block sunlight. We record ten reference spectra in this manner before and after each set of snow profile measurements. We later perform a linear interpolation between the two sets to obtain the reference spectrum specific to each measurement height, in order to account for spectrometer drift. We have observed a maximum drift of 8% in the mean intensity between 940 nm and 1020 nm over the course of 40 minutes. Laboratory testing shows this drift to be approximately linear in time, with a maximum error due to nonlinear drift of 1.4%.

Because the data processing technique uses the normalized integral of the absorption feature relative to the “continuum” spectrum, the grain size measurement is insensitive to changes in illumination. The exception to this would be if a significant spectral shift occurred in the light source between the time of Spectralon reflectance measurement and snow measurement. Even this would be somewhat minimized by the interpolation of the Spectralon measurements before and after snow measurements, which (assuming linear changes) accounts for spectrometer drift as well as light source drift.

2.4. Field operation

Fig. 3 shows a photograph of the profiler probe in operation. We first use an unmodified Federal snow sampler to remove a snow core and create a 50 mm diameter hole into which we insert the assembled sleeve (modified Federal sampler). In extremely loose or powdery snow, a flexible polycarbonate liner can be inserted into the sleeve prior to insertion into the snow to keep snow from falling into the viewing slots and accumulating at the bottom of the tube. After the sleeve is in place, the liner can be gently removed by pulling an attached cord. Probe performance may vary for different types of snow conditions such as depth hoar due to difficulties in drilling the initial hole. However, if care is taken to ensure a complete core (e.g. by obtaining a soil plug) the probe should perform adequately, as long as coring is

Table 1
Optical angles for different probe configurations.

	Fiber light	In-bore light	Contact probe
Incidence angle	28°	52°	23°
Reflected angle	-28°	-28°	32°

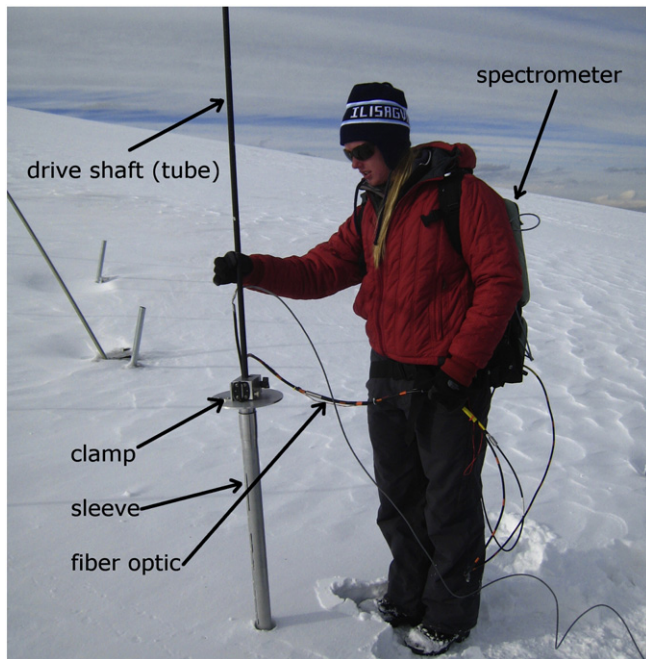


Fig. 3. Field operation—black tarp not shown.

possible. This is the case for most snowpacks, including depth hoar, unless unusually hard ice layers are present.

Once the sleeve is in place, we affix the clamping hardware to the top and insert the bore rider containing the optics. With the probe inside the sleeve but above the snow surface, we manually align the optics to the viewing slot in the sleeve and note the position of the slit on the camera's viewing screen. We then temporarily affix a Spectralon panel to the side of the sleeve, directly in front of the slit at the location of the probe optics and cover with the black tarp. We record reference spectra using the Spectralon panel, then move the probe below the snow surface and begin stepping the probe down by regular 2 cm intervals, clamping in place at each location to record snow spectra. After recording the full profile of snow spectra, we raise the probe above the surface again and record the second set of reference spectra with the Spectralon. Data processing occurs after fieldwork, and is discussed in a dedicated section below.

Depth measurements are made manually to 2 cm locational accuracy and spectra are automatically saved sequentially. Future versions of the probe will contain a motorized drive for lowering the optics into the snowpack as well as automated tracking of snowpack depth. During normal operation, recording a spectrum at each data point takes approximately 10 seconds, with another 10–20 seconds to move and lock at the next location. Thus, for a 2 m profile with 2 cm vertical sampling, the measurement takes roughly 5 minutes, not including the initial coring and spectralon measurements.

2.5. Contact probe

During field testing, snow-pit contact spectroscopy served as a baseline against which to compare data from the spectral profiler probe. The detailed procedure for these measurements is given by Painter et al. (2007b). We give a brief overview of the measurements here.

The contact probe is a commercially available unit from ASD, consisting of a hand-held fixture containing a halogen light source, which shines onto the sampling surface and a fiber optic cable which transmits reflected light to the spectrometer. A black standoff is affixed to the front of the contact probe to ensure consistent spacing when the standoff is touched to the snow surface, eliminate melting due to energy

that would be conducted by direct contact between probe and snow, and further shield the measurements from incident ambient light. The snow pit is covered with an opaque tarp with two meters of reach beyond the pit face (Painter et al., 2007b).

To obtain contact spectral profile data, we dig a snow pit to the ground-snow interface and record reflectance spectra at vertical spatial intervals by manually holding the probe up to the pit wall, then stepping down incrementally for each point in 2 cm increments. As with the profiler probe, calibration is accomplished using a Spectralon panel by recording 10 reference spectra before and after snow data collection and interpolating in time to account for spectrometer drift.

2.6. Data processing

The technique for retrieving snow grain size from spectral data is described in detail by Nolin and Dozier (2000) and Painter et al. (2007b). We give a brief overview here, which is not intended as a complete description of the method. The retrieval is based on comparison of experimentally collected spectra with theoretical reference spectra of idealized snow grains generated by the radiative transfer model DISORT. These retrievals have been validated in various settings, grain sizes, and grain shapes (Nolin and Dozier, 2000; Painter et al., 2003, 2007b; Painter and Dozier 2004). Taken further to the end goal of the present work, Painter et al. (2007b) constrained radiative transfer modeling of snow albedo with contact spectroscopy measures of grain size stratigraphy, reducing uncertainties to 8 W/m² in net shortwave flux.

The magnitude of the ice absorption feature with maximum near 1030 nm is sensitive to grain size (Fig. 4). To eliminate sensitivity to changes in illumination conditions, the integral of the continuum-normalized spectrum across the feature is used, as opposed to using the absolute reflectance at any particular wavelengths. The integral of the reflectance across the absorption feature is normalized to the “continuum” reflectance, represented graphically on the spectrum by a straight line connecting the shoulders of the absorption feature, from 950 nm to 1090 nm. Thus the integral value is obtained by:

$$I_{1030 \text{ nm}} = \int_{950 \text{ nm}}^{1090 \text{ nm}} \frac{R_c - R_s}{R_c} d\lambda \approx \sum \frac{R_c - R_s}{R_c} \quad (2)$$

where R_c is the “continuum” reflectance, and R_s is the actual measured reflectance in the absorption feature. We can then compare the value of $I_{1030 \text{ nm}}$ for experimentally collected spectra to theoretical spectra of known grain size. Fig. 5 shows theoretical spectra for the two different probe geometries (for the same uniform grain size), along with

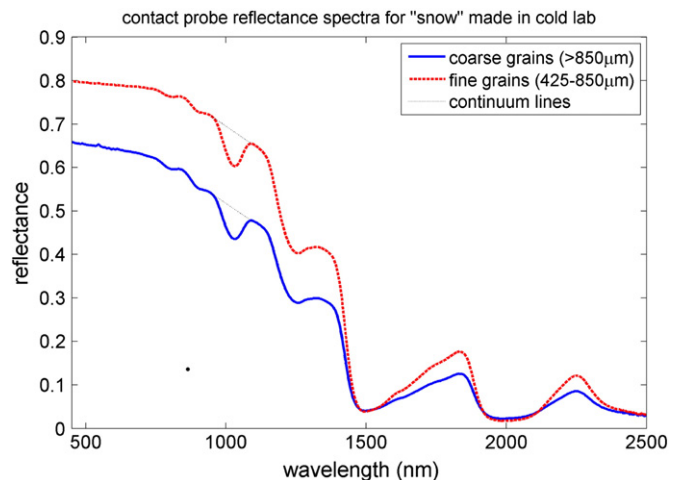


Fig. 4. Spectra of coarse and fine grains. These grains were made by breaking up ice in a cold lab then sifting through sieves to obtain specific ranges of physical grain size.

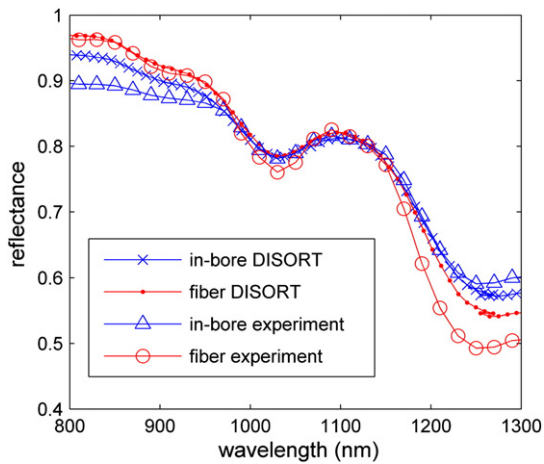


Fig. 5. Modeled spectra from DISORT and experimental spectra for the two probe geometries.

experimental spectra scaled to remove the effect of slight illumination changes.

To generate the theoretical spectra, the DISORT code (Stamnes et al., 1988) provides the discrete ordinates solution to the integro-differential radiative transfer equation, simulating the radiative transfer through a homogeneous snowpack comprised of spherical grains of pure ice of a particular grain size with the specified illumination/reflection geometry of the contact probe or profiler probe. From the modeled spectra, we generate a lookup table of the integral value vs. grain size, which can be interpolated to find the OGD that best matches the value of $I_{1030\text{ nm}}$ for the experimentally measured spectrum. Given that the OGD is derived from the integral of the normalized reflectance continuum, the retrieval is not sensitive to the distance of the illumination source and target or the source intensity.

Three separate lookup tables are used here, to account for the differing geometry of the two probe configurations (in-bore light and fiber light) and the contact probe. In the generation of each table, the ideal spectra are generated using the appropriate incidence and reflectance angles for each configuration as inputs into the DISORT model. Each lookup table is then used to obtain the grain size from the spectra taken with the corresponding instrument.

3. Field test results

Two field campaigns in winter and spring of 2010 provided testing for the prototype profiler probe at Storm Peak Laboratory (SPL) in Steamboat Springs, CO and Niwot Ridge, CO. The SPL site (3220 m elevation; 40.455° N, -106.744° W) is located in alpine terrain near the top of Steamboat Ski Resort. The Niwot site (3528 m; 40.057° N, 105.589° W and surrounding area) consisted of several study areas in alpine and subalpine terrain. During both campaigns, nearby snow pits provided data from contact spectroscopy and hand lens measurements for comparison with profiler probe data. Whenever possible, these pits were excavated such that the pit wall for the contact spectroscopy profile coincided with the same vertical plane as the profiler probe measurement. Within this plane, the contact probe profile was generally 10–20 cm lateral distance from the line of the profiler probe data. When this was not possible, data were compared with the nearest snowpit data available, no more than 5 m away.

3.1. Storm Peak Lab field campaign

For the SPL field campaign, February 18–22, 2010, measurements were taken at several points within a 15 × 15 m protected area located on the west side of the laboratory building (Fig. 6). The SPL campaign employed only the fiber light configuration of the probe, as this was

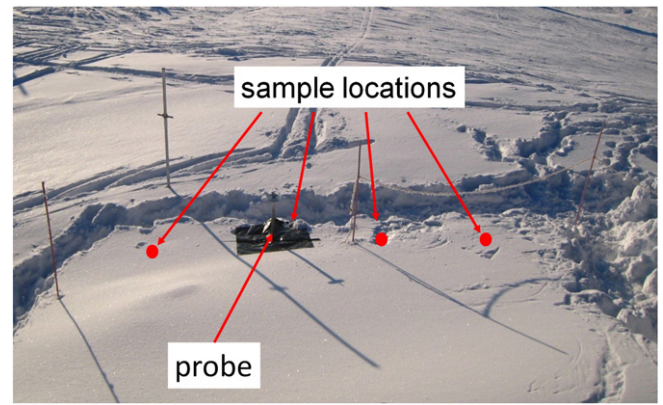


Fig. 6. SPL field site showing transect locations.

prior to the construction of the in-bore light hardware. Ten profiles of grain size were recorded with the profiler probe at various locations within the study plot, including a transect of four points across the western edge of the plot. Six snow pits were excavated for stratigraphy measurements with traditional hand lens and contact spectroscopy. Note that this area partially contains a drift, which likely influences the spatial variability.

Fig. 7 (left panel) shows a plot of the grain size vs. depth from the profiler probe for each of the transect locations, which generally shows an increase in grain size with depth, as is typical for a midwinter Rocky Mountain snowpack. The data also show significant variation in the lateral direction (from profile to profile), with some profiles showing sharp increases in grain size around 20 cm depth. The lateral standard deviation between profiles varies from a minimum of 108 μm at 84 cm to a maximum of 822 μm at 21 cm. Assuming these peaks are indeed physical, such lateral heterogeneity is not uncommon, especially in snowpacks influenced by surface irregularities, which are present in all but the flattest terrain (Birkeland, 2001).

Fig. 7 (center panel) shows a plot of the average grain size from the profiler probe for the transect data, along with a mean profile from two columns of contact spectroscopy data from a nearby snow pit approximately 1.5 m away. The two instruments agree with an average RMSE of 110 μm , including the large grain layers deep in the snowpack, where the profiler probe retrieves significantly larger grain sizes than the contact probe (up to factor of two). Two possible explanations exist for this discrepancy. The first possibility is associated with lateral variability in the snowpack, meaning that the very large grain layer simply does not exist at the location of the contact spectroscopy measurements. As Fig. 7 shows, there is wide variability in this layer between profile locations, with some profiles completely lacking the larger grain sizes at the base of the snowpack. This again highlights the importance of obtaining many profiles to characterize the lateral heterogeneity of the snowpack.

Alternatively, the discrepancy may be due to the difference in optical setup between the two instruments. The fiber light configuration, used in this field campaign, illuminates and views a spot size of approximately 4 mm, while the pit-based contact probe illuminates an approximately 30 mm spot and views a 21 mm spot. Although the light likely propagates a few centimeters into the snow for both configurations (thus creating a sample volume larger than the spot size), this larger field of view may result in measurements which integrate several thin layers of varying grain sizes, effectively averaging out the scattering of very thin layers of large grains. This effect may be enhanced by the disturbance of snow pit excavation, which can transport grains between layers on the pit face. Conversely, when considered in the context of Mie scattering, a small spot illumination size, approaching the grain size, can lead to inadequate capture of the surface scattering from large grains compared to the volume scattering component. This would lead to overestimation of grain size, and the effect would be most significant

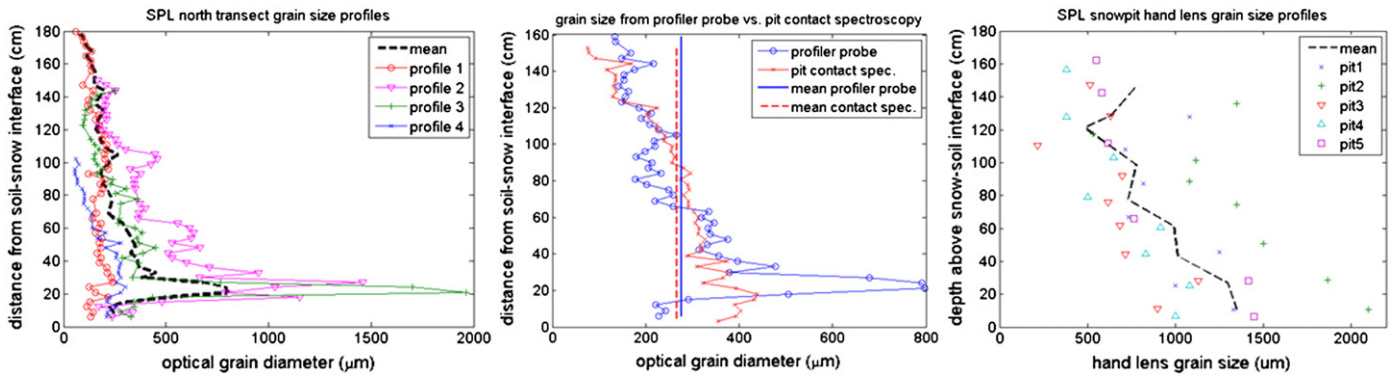


Fig. 7. Left: profiler probe transect grain size profiles. Center: mean transect profile vs. snow-pit contact spectroscopy. Right: hand lens profile measurements. Dotted lines represent mean values.

in regions of large grains. Further study is necessary to determine the relative influence of these effects.

Fig. 7 (right panel) also shows hand lens grain size estimation from all five of the SPL snow pits. Note that hand lens measurements are useful for qualitative insights only, as they do not necessarily correlate with optical grain size. These data show a general increase in grain size with depth from the surface, with some of the pits showing a gradual rise in grain size from surface to soil, and others showing sharp increases at a particular depth. This supports the profiler probe observations of lateral heterogeneity, and shows the same general trend as the optical grain size measured by the profiler probe and contact probe. Furthermore, the measurements showed that the lateral range in grain size values increases with depth, from a standard deviation of 87 μm near the surface, to 475 μm near the bottom. This further supports the hypothesis that snowpack lateral variability is responsible for a large part of the discrepancies between the profiler probe and contact probe.

3.2. Niwot Ridge field campaign

The Niwot Ridge campaign in early May 2010 included measurements at several locations within each of two remote sites: an alpine site (3517 m elevation), and a subalpine site near timberline (3367 m elevation). Fig. 8 (left panel) shows the calculated grain size profiles for both probe configurations, along with contact probe snow-pit data. Unfortunately, the fiber light configuration data did not penetrate to the ground due to a mechanical jam. However, we include the dataset here because this location showed the greatest grain size variation with depth, and comparison of the in-bore light configuration with the contact probe provides useful data.

Fig. 8 (center) shows the grain size profiles from a second alpine site, approximately 500 m from the first site at similar elevation, and

Fig. 8 (right) shows the profiles for the subalpine site. In all three of these figures, the profiler probe data appear to follow the same trend as the contact probe (approximately 20 cm lateral distance away for all three), but the fiber light configuration underpredicts the grain size by an average of 30% and the in-bore light configuration overpredicts grain size by an average of 60%. In part, this is potentially due to melting of the snow grains upon exposure to heating by the halogen light source, used with the in-bore light configuration and the contact probe. This is an artifact of most approaches that use contact spectroscopy in snow. As the light source is held near the snow, the thermal irradiance from the bulb and its mount heats the snow and increases the grain size. All efforts are made to minimize this by holding the light source to the snow for as short a time as possible, usually 2–5 seconds for adequate data acquisition for the contact spectroscopy and 5–10 seconds for the in-bore probe.

As the grains melt, the apparent OGD grows, as shown in Fig. 9, but the effect over a span of 20 seconds causes grain size to increase by only ~50 μm and ~25 μm in the in-bore and contact spectroscopy cases, respectively. These temporal changes in grain size may explain some of the differences in the techniques but the large differences shown in Fig. 8 (right) likely result from additional factors as mentioned previously. To collect the data in this figure, the probe was held in one location, and spectra were collected every few seconds. The effect is enhanced for the in-bore light probe because the halogen bulb is located closer to the snow surface and confined within the small diameter sleeve, thus concentrating more energy into the snowpack. The fiber light configuration keeps the halogen bulb more remotely located from the sampling area, and little thermal radiation transmits through the fiber to reach the snow. For the Niwot Ridge data, the temperature of the spring snowpack was close to melting, thus enhancing thermal effects.

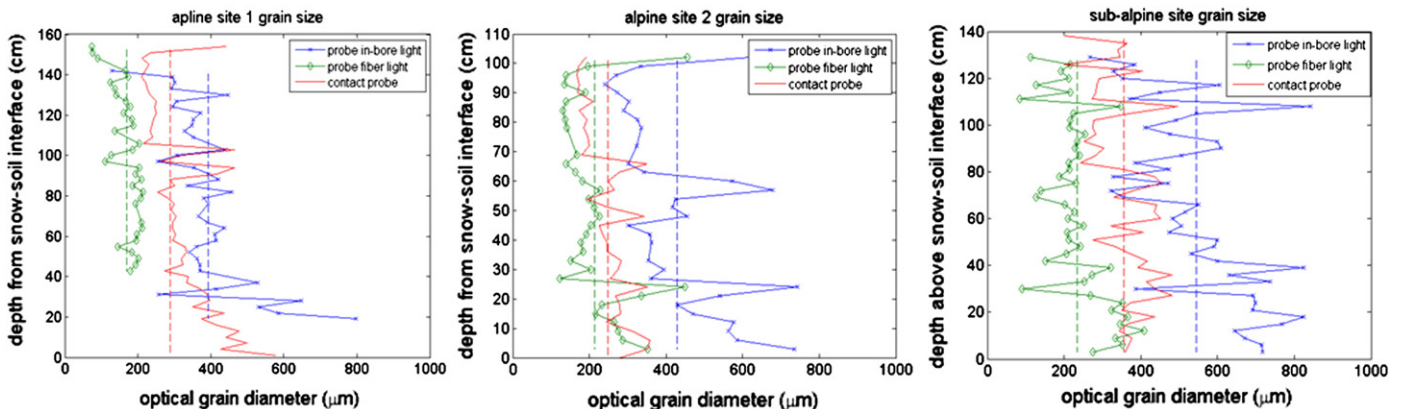


Fig. 8. Grain size profiles for in-bore and fiber light probe configurations along with pit contact spectroscopy. Left: alpine site 1. Center: alpine site 2. Right: subalpine site. Dotted lines represent mean values for each profile of corresponding color.

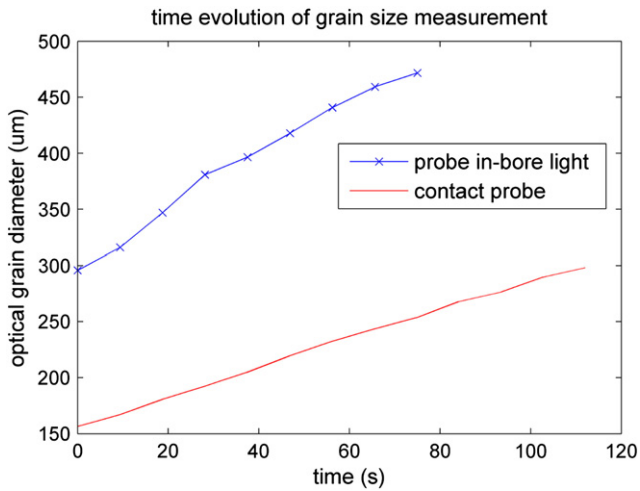


Fig. 9. OGD growth when exposed to halogen heat source. These data are taken with the probe fixed at one location approximately 30 cm into the snowpack.

Fig. 10 shows two successive grain size profiles from a single sample location from the in-bore light probe, separated by approximately 15 minutes in time. This plot shows the repeatability of the probe for estimating grain size, as the average of the difference between the two profiles is only 4%. This compares well with contact spectroscopy, which upon repeat passes, has differences of 6%. Note, however, that most of the grain sizes from the second pass of the in-bore light probe are systematically slightly larger than those from the first pass. Thus it is likely that a small amount of melting has occurred between the passes. This reinforces the idea that light-source-induced melting is only a small contributor to the differences in the techniques, even in the near 0 °C spring snowpack.

4. Discussion

The above results demonstrate the functionality of the spectral profiler probe, and show promise for its use in conjunction with remote sensing data. The results also reveal many of the inherent difficulties with ground-based point measurements of grain size, which, as we show, exhibits considerable lateral variability. This large lateral variability

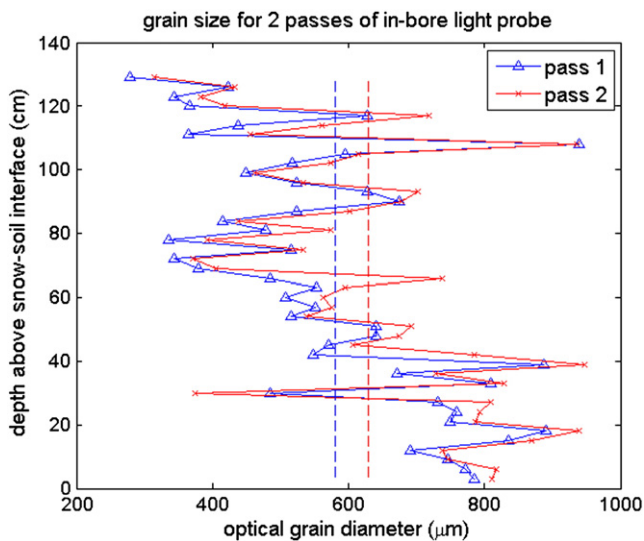


Fig. 10. Successive profiles with in-bore light showing repeatability with average 4% difference, with slight growth in the second profile.

is common in most mountain snowpacks, and therefore a single profile poorly captures the average grain size profile. Hence, acquiring many vertical profiles in a given region is important because remote passive microwave or radar instruments are sensitive to the sub-pixel variability in grain size profiles (Harper and Bradford, 2003). The instrument described here, when fully matured, provides a means to obtain the data necessary for these purposes.

Insertion-type probes such as POSSSUM (Arnaud et al., 2011) and our spectral profiler probe substantially decrease snowpack disturbance by limiting exposure to the ambient atmospheric heating and diffuse irradiance from leaked light and snow-pit faces. Mechanical disturbance, however, is not completely eliminated. Observations from POSSSUM indicate grinding of large grains into smaller grains by the action of the rotating power drilling device used to create the hole (Picard et al., 2010). This effect may be smaller with the manual Federal sampler used here for drilling, however some amount of disturbance is inevitable, especially when the device must break through very hard layers. Also to be noted is the possibility of compressing the snow with the insertion probe. We expect this effect to be small, since a core is removed and the sleeve inserted into the empty hole, thus the amount of snow that is displaced (or compressed) into the surrounding snowpack is relatively small.

The field testing results also show the effect of snow grain metamorphism due to the application of external heating from the spectrometer light source. We expect this effect to be most severe for snow comprised of crystalline or other complex geometric grain shapes, which can be easily metamorphosed to larger OGD shapes with small amounts of energy input, and also for warmer snowpacks near the melting point. By using the external light source configuration, this effect is minimized compared to the in-bore light and contact spectroscopy. Most contact probe measurements are made in less than 5 seconds, and around 10 seconds for the profiler probe. As Fig. 9 shows, this corresponds to 3% and 7% growth for the contact probe and in-bore light profiler probe, respectively. This is much less than the observed difference between the mean grain size measurements, therefore this effect alone is clearly not sufficient to explain the difference in grain size measured by the two methods.

The spectral profiler device shows promise for satellite SWE retrieval applications and for constraining physical snow models (e.g. Lehning et al., 2006). Until passive and active microwave SWE retrieval techniques mature, they will rely upon ground-based datasets to provide grain-size distribution data for algorithm development and validation (Durand and Margulis, 2006; Durand et al., 2008a, 2008b). Currently, grain size retrievals for input into various models are extrapolated spatially and temporally from limited snow-pit measurements or remote measurements of the surface layer (Green and Dozier, 1996; Molotch and Bales, 2006; Nolin and Dozier, 2000; Painter et al., 2003). The type of instrument presented here provides a small step toward the delivery of large, easily-obtainable datasets of grain size profiles over representative geographical areas.

Acknowledgments

This work was performed in part at the Jet Propulsion Laboratory, California Institute of Technology, under a contract with the National Aeronautics and Space Administration. The probe development was funded by the NASA Terrestrial Hydrology Program under contracts NNX08AH18G and NNX09AM10G. Part of T. H. Painter's work was funded by NASA grant NNX10A097G, and M. Durand's contribution was funded by NASA grant NNX09AM10G. The purchase of the ASD field spectrometer was made possible by NSF grant EAR-0744542. We thank Ian McCubbin and Gannet Hallar of Storm Peak Laboratory for their support and use of the Storm Peak Lab facilities. We also thank Jennifer Petrzalka, Ty Atkins, and Alexandra Arnsten for their assistance and organization of field work and data collection, as well as Kevin Hand and Greg Okin for use of equipment and insightful discussions.

References

- American Avalanche Association, 2004. Snow, Weather, and Avalanches: Observational Guidelines for Avalanche Programs in the United States. American Avalanche Association.
- Arnaud, L., Picard, G., Champollion, N., Domine, F., Gallet, J.C., Lefebvre, E., Fily, M., Barnola, J.M., 2011. Measurement of vertical profiles of snow specific surface area with a 1 cm resolution using infrared reflectance: instrument description and validation. *Journal of Glaciology* 57 (201), 17–29.
- Bales, R.C., Molotch, N.P., Painter, T.H., Dettinger, M.D., Rice, R., Dozier, J., 2006. Mountain hydrology of the western United States. *Water Resources Research* 42 (8), 8432.
- Birkeland, K.W., 2001. Spatial patterns of snow stability throughout a small mountain range. *Journal of Glaciology* 47 (157), 176–186.
- Brucker, L., Picard, G., Arnaud, L., Barnola, J.-M., Schneebeli, M., Lefebvre, E., Fily, M., 2011. Modeling time series of microwave brightness temperature at Dome C, Antarctica, using vertically resolved snow temperature and microstructure measurements. *Journal of Glaciology* 57 (201), 171–182.
- Bruegge, C., Chrien, N., Haner, D., 2001. A spectralon BRDF data base for MISR calibration applications. *Remote Sensing of Environment* 77 (3), 354–366.
- Brzoska, J.B., Flin, F., Lesaffre, B., Coleou, C., Lambole, P., Delesse, J.F., Saÿc, B.L., Vignoles, G., 2001. Computation of the surface area of natural snow 3D images from x-ray tomography: two approaches. *Image Analysis & Stereology* 20 (Suppl. 1), 306–312.
- Chang, A.T.C., Foster, J.L., Hall, D.K., Rango, A., Hartline, B.K., 1982. Snow water equivalent estimation by microwave radiometry. *Cold Regions Science and Technology* 5 (3), 259–267.
- Chen, S., Baker, I., 2010. Evolution of individual snowflakes during metamorphism. *Journal of Geophysical Research D: Atmospheres* 115, 1–9.
- Domine, F., Albert, M., Huthwelker, T., Jacobi, H., Kokhanovsky, A., Lehning, M., Picard, G., Simpson, W., 2008. Snow physics as relevant to snow photochemistry. *Atmospheric Chemistry and Physics* 8 (2), 208.
- Dozier, J., Green, R.O., Nolin, A.W., Painter, T.H., 2009. Interpretation of snow properties from imaging spectrometry. *Remote Sensing of Environment* 113, S25–S37.
- Durand, M., Margulis, S.A., 2006. Feasibility test of multifrequency radiometric data assimilation to estimate snow water equivalent. *Journal of Hydrometeorology* 7 (3), 443–457.
- Durand, M., Kim, E.J., Margulis, S.A., 2008a. Quantifying uncertainty in modeling snow microwave radiance for a mountain snowpack at the point-scale, including stratigraphic effects. *IEEE Transactions on Geoscience and Remote Sensing* 46 (6), 1753–1767.
- Durand, M., Molotch, N.P., Margulis, S.A., 2008b. Merging complementary remote sensing datasets in the context of snow water equivalent reconstruction. *Remote Sensing of Environment* 112 (3), 1212–1225.
- Fierz, C., Armstrong, R.L., Durand, Y., Etchevers, P., Greene, E., McClung, D.M., Nishimura, K., Satyawali, P.K., Sokratov, S.A., 2009. The International Classification for Seasonal Snow on the Ground. IHP-VII Technical Documents in Hydrology N°83, IACS Contribution N°1. UNESCO-IHP, Paris.
- Flanner, M.G., Zender, C.S., Randerson, J.T., Rasch, P.J., 2007. Present-day climate forcing and response from black carbon in snow. *Journal of Geophysical Research* 112, D11202.
- Flanner, M.G., Zender, C.S., Hess, P.G., Mahowald, N.M., Painter, T.H., Ramanathan, V., Rasch, P.J., 2009. Springtime warming and reduced snow cover from carbonaceous aerosols. *Atmospheric Chemistry and Physics* 9 (7), 2481–2497.
- Foster, J.L., Chang, A.T.C., Hall, D.K., 1997. Comparison of snow mass estimates from a prototype passive microwave snow algorithm, a revised algorithm and a snow depth climatology. *Remote Sensing of Environment* 62 (2), 132–142.
- Foster, J.L., Sun, C., Walker, J.P., Kelly, R., Chang, A., Dong, J., Powell, H., 2005. Quantifying the uncertainty in passive microwave snow water equivalent observations. *Remote Sensing of Environment* 94 (2), 187–203.
- Gallet, J.C., Domine, F., Zender, C.S., Picard, G., 2009. Measurement of the specific surface area of snow using infrared reflectance in an integrating sphere at 1310 and 1550 nm. *The Cryosphere* 3 (2), 167–182.
- Green, R.O., Dozier, J., 1996. Retrieval of surface snow grain size and melt water from AVIRIS spectra. Summaries of the Sixth Annual JPL Airborne Earth Science Workshop NASA no. 19980201639.
- Grenfell, T.C., Warren, S.G., 1999. Representation of a nonspherical ice particle by a collection of independent spheres for scattering and absorption of radiation. *Journal of Geophysical Research* 104 (D24), 31697–31709.
- Harper, J.T., Bradford, J.H., 2003. Snow stratigraphy over a uniform depositional surface: spatial variability and measurement tools. *Cold Regions Science and Technology* 37 (3), 289–298.
- Kelly, R.E., Chang, A.T., Tsang, L., Foster, J.L., 2003. A prototype AMSR-E global snow area and snow depth algorithm. *IEEE Transactions on Geoscience and Remote Sensing* 41 (2), 230–242.
- Kerbrat, M., Pinzer, B., Huthwelker, T., Gaeggeler, H.W., Ammann, M., Schneebeli, M., 2008. Measuring the specific surface area of snow with X-ray tomography and gas adsorption: comparison and implications for surface smoothness. *Atmospheric Chemistry and Physics* 8 (5), 1261–1275.
- Langlois, A., Royer, A., Montpetit, B., Picard, G., Brucker, L., Arnaud, L., Harvey-Collard, P., Fily, M., Goita, K., 2010. On the relationship between snow grain morphology and in-situ near infrared calibrated reflectance photographs. *Cold Regions Science and Technology* 61 (1), 34–42.
- Legagneux, L., Cabanes, A., Dominé, F., 2002. Measurement of the specific surface area of 176 snow samples using methane adsorption at 77 K. *Journal of Geophysical Research* 107, 4335–4350.
- Lehning, M., Volksch, I., Gustafsson, D., Nguyen, T., Stähli, A., Zappa, M., 2006. ALPINE3D: a detailed model of mountain surface processes and its application to snow hydrology. *Hydrological Processes* 20, 2111–2128.
- Marshall, H.P., Schneebeli, M., Koh, G., 2007. Snow stratigraphy measurements with high-frequency FMCW radar: comparison with snow micro-penetrometer. *Cold Regions Science and Technology* 47 (1–2), 108–117.
- Matzl, M., Schneebeli, M., 2006. Measuring specific surface area of snow by near-infrared photography. *Journal of Glaciology* 52 (179), 558–564.
- Matzl, M., Schneebeli, M., 2010. Stereological measurement of the specific surface area of seasonal snow types: comparison to other methods, and implications for mm-scale vertical profiling. *Cold Regions Science and Technology* 64, 1–10.
- Molotch, N.P., Bales, R.C., 2006. Comparison of ground-based and airborne snow surface albedo parameterizations in an alpine watershed: impact on snowpack mass balance. *Water Resources Research* 42 (5), W05410.
- National Research Council, 2007. Earth Science and Applications from space: National Imperatives for the Next Decade and Beyond. The National Academies Press, Washington, D.C.
- Nolin, A.W., 2010. Recent advances in remote sensing of seasonal snow. *Journal of Glaciology* 56 (200), 1141.
- Nolin, A.W., Dozier, J., 2000. A hyperspectral method for remotely sensing the grain size of snow. *Remote Sensing of Environment* 74 (2), 207–216.
- Painter, T., Dozier, J., 2004. Measurements of the hemispherical-directional reflectance of snow at fine spectral and angular resolution. *Journal of Geophysical Research* 109, D18115.
- Painter, T.H., Dozier, J., Roberts, D.A., Davis, R.E., Green, R.O., 2003. Retrieval of subpixel snow-covered area and grain size from imaging spectrometer data. *Remote Sensing of Environment* 85 (1), 64–77.
- Painter, T.H., Barrett, A.P., Landry, C.C., Neff, J.C., Cassidy, M.P., Lawrence, C.R., McBride, K.E., Farmer, G.L., 2007a. Impact of disturbed desert soils on duration of mountain snow cover. *Geophysical Research Letters* 34, 1–6.
- Painter, T.H., Molotch, N.P., Cassidy, M., Flanner, M., Steffen, K., 2007b. Contact spectroscopy for determination of stratigraphy of snow optical grain size. *Journal of Glaciology* 53 (180), 121–127.
- Picard, G., Arnaud, L., Champollion, N., Domine, F., Fily, M., Dec. 2010. Deep profiles of snow specific surface area at Dome C, Antarctica, and application to passive microwave remote sensing. AGU Fall Meeting Conference Presentation, San Francisco, CA.
- Rott, H., Yueh, S., Cline, D., Duguay, C., Essery, R., Haas, C., Heliere, F., Kern, M., Macelloni, G., Malnes, E., et al., 2010. Cold regions hydrology high-resolution observatory for snow and cold land processes. *Proceedings of the IEEE* 98 (5), 752–765.
- Shi, J., Dozier, J., 2000. Estimation of snow water equivalence using SIR-C/X-SAR. II. Inferring snow depth and particle size. *IEEE Transactions on Geoscience and Remote Sensing* 38 (6), 2475–2488.
- Stamnes, K., Tsay, S., et al., 1988. Numerically stable algorithm for discrete-ordinate-method radiative transfer in multiple scattering and emitting layered media. *Applied Optics* 27 (12), 2502–2509.
- Warren, S.G., 1982. Optical properties of snow. *Reviews of Geophysics* 20 (1), 67–89.